

Photoinduced Electron-Transfer Processes of Fullerene (C_{60}) with Amine Donors: Excited Triplet Route vs Excited Singlet Route

Atula S. D. Sandanayaka, Yasuyuki Araki, Chuping Luo,† Mamoru Fujitsuka,†† and Osamu Ito*

Institute of Multidisciplinary Research for Advanced Materials, Tohoku University, Katahira 2-1-1, Aoba-ku, Sendai 980-8577

Received January 16, 2004; E-mail: ito@tagen.tohoku.ac.jp

Dynamic quenching processes of the excited states of C_{60} with amine donors have been studied by changing donor strength, donor concentration, and solvent polarity using steady-state and transient absorption and fluorescence spectroscopic techniques. Fluorescence quenching of C_{60} by amines was observed, which suggests a dynamic quenching process via the excited singlet state of C_{60} ($^1C_{60}$*) in polar and nonpolar solvents. In polar solvents, electron transfer via the excited triplet state of C_{60} ($^3C_{60}$*) producing radical ions ($C_{60}^{\bullet-}$ and amine$^{\bullet+}$) was observed by the nanosecond laser flash photolysis (ca. 6 ns laser pulse). When the donor concentrations are below 10–20 mmol dm^{-3}, the concentrations of the radical ions increased with the donor concentrations. With further increase of the concentrations of the donors up to 100 mmol dm^{-3}, on the other hand, the yields of the radical ions generated via $^3C_{60}$* decreased. These findings indicate that dynamic quenching of $^1C_{60}$* by amines increases with donor concentrations, resulting in a decrease of the intersystem crossing path to $^3C_{60}$*; thus, the yields of the radical ions generated via $^3C_{60}$* decreased even in the highly polar solvent. This implies that the radical ions generated by the dynamic quenching of $^1C_{60}$* may be quite short-lived, even in polar solvents, compared with the radical ions via $^3C_{60}$*.

Structures and reactivities of fullerenes have attracted considerable attention in a variety of research areas.[1,2] Fullerenes have high electron affinities and thus readily form anions by electrochemical reduction.[3,4] Especially, photo-excited fullerenes act as good electron acceptors in the presence of electron donors.[5–15] The contribution of the excited states of C_{60} to electron transfer can be controlled by the donor strength, donor concentration, and solvent polarity.[7–12] In the presence of relatively low concentrations of electron donors in polar solvents, photoinduced electron transfer occurs via the excited triplet state of C_{60} ($^3C_{60}$*), yielding long-lived free radical ions.[12–18] Thermodynamically, electron transfer via the excited singlet state of C_{60} ($^1C_{60}$*) is possible for the amine donors in various solvents. Usually, however, the electron-transfer via $^1C_{60}$* needs higher donor concentration ([D]) than that via $^3C_{60}$*, because the electron-transfer rate via $^1C_{60}$* (k_{et}^S[D]) has to be comparable with or larger than the intersystem crossing rate constant ($k_{ISC} = (7.7–8.3) \times 10^8$ s^{-1}),[19–23] while the electron-transfer rate via $^3C_{60}$* (k_{et}^T[D]) competes with the slow decay rate of $^3C_{60}$* ($k_T = (2–5) \times 10^4$ s^{-1}).[11,24] Thus, if k_{et}^S is close to the diffusion controlled limit (k_{diff}), electron transfer via $^1C_{60}$* becomes apparent for the donor concentrations higher than 10–20 mmol dm^{-3}.[7,9] Therefore, it is quite interesting to investigate the competitive paths in the photoinduced electron transfer from $^1C_{60}$* with that from $^3C_{60}$* by changing the donor strength, concentrations, and solvent polarity.

In the present study, we employed C_{60} and amines as electron acceptor and donors, respectively. These systems make it possible to excite selectively the acceptor (C_{60}) by the 532 nm laser light, avoiding complexity of interpretation due to the direct photo-ejection of electrons with the excitation of amine donors. In addition, the absorption band of $^3C_{60}$* appears at 740 nm,[11,12] which does not overlap with that of the radical anion of C_{60} ($C_{60}^{\bullet-}$ at 1080 nm).[13–17] By employing the aromatic and aliphatic amine donors in Fig. 1, the transient absorption bands of the radical cations would be anticipated to appear in the wavelength region shorter than 650 nm, which does not disturb the precise kinetic analyses of the transient absorption bands of $^3C_{60}$* and $C_{60}^{\bullet-}$ at 740 and 1080 nm, respectively.

From the time profiles of the transient absorptions of $^3C_{60}$* and $C_{60}^{\bullet-}$ in the visible and near-IR regions, in addition to the precise steady-state absorption and fluorescence spectra, we

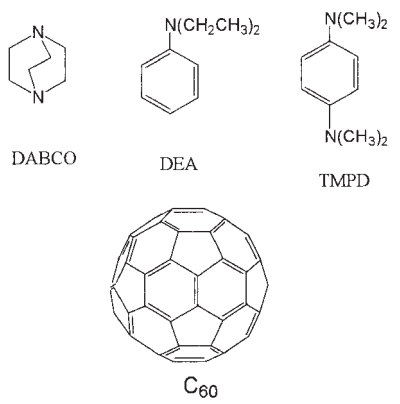

Fig. 1. Molecular structures and abbreviations.

† Present address: Georgetown University, Washington DC, 20057, USA

†† Present address: The Institute of Scientific and Industrial Research, Osaka University, Osaka

Published on the web July 9, 2004; DOI 10.1246/bcsj.77.1313

discussed the effects of donor strength, concentration, and solvent polarity on the bimolecular electron transfer process. We also found here that the generation of $C_{60}^{\bullet-}$ via $^3C_{60}$* gradually decreased with an increase in the donor concentration higher than 10–20 mmol dm^{-3}.

Experimental

Materials. C_{60} (>99.9%) was purchased from Texas Fullerene Corp. Commercially available *N*,*N*-diethylaniline (DEA; Tokyo Kasei Kogyo Co. Ltd), 1,4-diazabicyclo[2.2.2]octane (DABCO; Kanto Chemical Co. Inc.), and *N*,*N*,*N*′,*N*′-tetramethyl-*p*-phenylenediamine (TMPD; Aldrich Chemicals) were used after purifications; they were purified by distillation, recrystallization, and sublimation, respectively. All solvents were spectroscopic or HPLC grade.

Spectral Measurements. Nanosecond transient absorption measurements were carried out using SHG (532 nm) of a Nd:YAG laser (Spectra-Physics, Quanta-Ray GCR-130, fwhm 6 ns) as an excitation source. For transient absorption spectra in the near-IR region (600–1200 nm), monitoring light from a pulsed Xe lamp was detected with a Ge-avalanche photodiode (Hamamatsu Photonics, B2834). Photoinduced events in micro- and millisecond time regions were measured using a continuous Xe lamp (150 W) and an InGaAs-PIN photodiode (Hamamatsu Photonics, G5125-10) as a probe light and a detector, respectively. Details of the transient absorption measurements were described elsewhere.[16,17] All the samples in a quartz cell (1 × 1 cm) were deaerated by bubbling Ar gas through the solution for 15 min. Steady-state absorption spectra in the visible and near-IR regions were measured on a JACSO V570 DS spectrometer. Fluorescence spectra were measured on a Shimadzu RF-5300PC spectro-fluorophotometer.

Electrochemical Measurements. The cyclic voltammetry measurements were performed on a BAS CV-50 W electrochemical analyzer in deaerated benzonitrile (BN) or *o*-dichlorobenzene (DCB) solution containing 0.10 M tetrabutylammonium hexafluorophosphate (Bu_4NPF_6) as a supporting electrolyte at 100 mV s^{-1} of scan rate. A conventional three-electrode cell employing Pt-working and counter electrodes and an Ag/AgCl reference electrode was used for the measurements. The redox potentials were evaluated vs ferrocene/ferrocenium ion (Fc/Fc^+) as an internal standard.

Results and Discussion

Steady-State Absorption and Fluorescence Studies. Absorption spectra of C_{60} and the donors were recorded from 400 to 900 nm by changing the donor concentration (Fig. 2). In the longer wavelength region (>420 nm), C_{60} showed absorption bands with peaks at 540 and 595 nm. The shapes of the absorption bands did not change significantly on the addition of excess DEA and TMPD,[25] denying the existence of appreciable charge-transfer interaction in the ground state.[26]

Steady-state fluorescence spectra are also shown in Fig. 2; fluorescence peaks of C_{60} appeared at 695 and 725 nm. Fluorescence intensity of C_{60} decreased with an increase in the concentration of DEA or TMPD without appreciable change in the spectral shape of the main fluorescence peak region (650–800 nm). On the addition of 100 mmol dm^{-3} of DEA or TMPD in toluene, the fluorescence intensity of C_{60} at the peak decreased by a factor of 1/3 or 1/5, respectively. No new fluorescence band was observed in the 650–800 nm region. Addition of DABCO also showed a similar behavior. These findings suggest that the exciplex formation is rare between $^1C_{60}$* and amine donors less than 100 mmol dm^{-3}, which is in good agreement with the recently reported results.[24] In Fig. 2, the weak fluorescence remained around 620 and 820 nm on addition of high concentration of DEA or TMPD, which may be related to the scattered light.

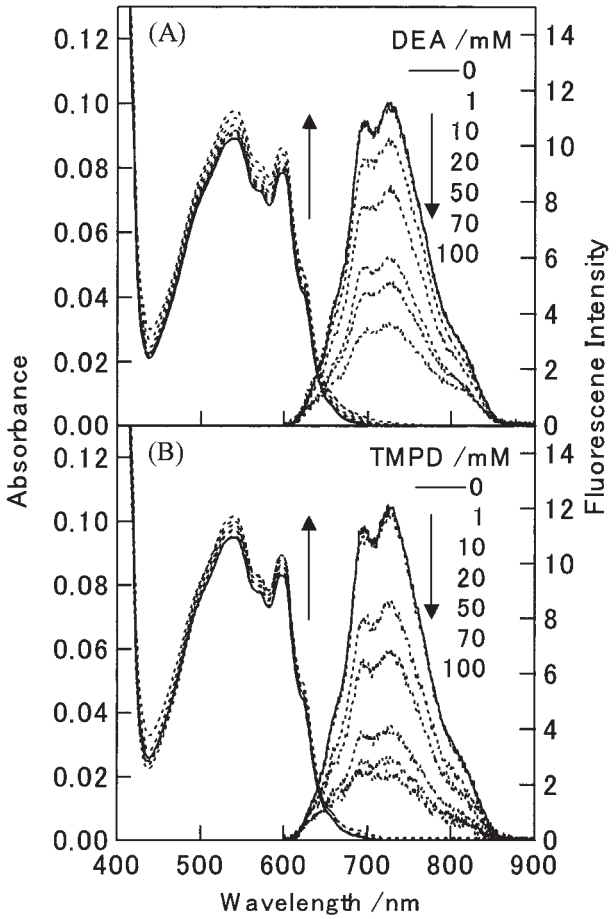

Fig. 2. Steady-state absorption and fluorescence spectra of C_{60} (0.1 mmol dm^{-3}) in the presence of (A) DEA and (B) TMPD in toluene (mM = mmol dm^{-3}).

Stern–Volmer plots for the fluorescence intensities of C_{60} in the presence of amine gave straight lines, as shown in Fig. 3. The observed linear relationships indicate that dynamic quenching of $^1C_{60}$* predominantly occurs without formation of charge-transfer complex in the ground state. From the Stern–Volmer plots, the fluorescence quenching rate-constants (k_q^S) can be evaluated using Eq. 1 and the reported intrinsic singlet decay rate constant (k_0^S) for C_{60}:[22]

$$I_{f0}/I_f = 1 + (k_q^S/k_0^S)[D], \quad (1)$$

where I_{f0} and I_f refer to the fluorescence intensities in the absence and presence of amine donors (D), respectively. The evaluated k_q^S values for dynamic quenching of $^1C_{60}$* by DEA, DABCO, and TMPD in various solvents are listed in Table 1. In each solvent, the k_q^S values for DABCO, which is an aliphatic bulky amine with high oxidation potential (E_{ox}),

are smaller than those for aromatic amines with low E_{ox} values (Table 1). Among the aromatic amines, the k_q^S values for TMPD are larger than the corresponding values of DEA. The order of the k_q^S values is in accord to the donor strength of amines, which is evaluated from the E_{ox} values of donors in BN and DCB. In each amine donor, the k_q^S values tend to increase with the decrease in the solvent viscosity rather than the solvent polarity, suggesting that the fluorescence quenching processes occur near diffusion-controlled limits.[27]

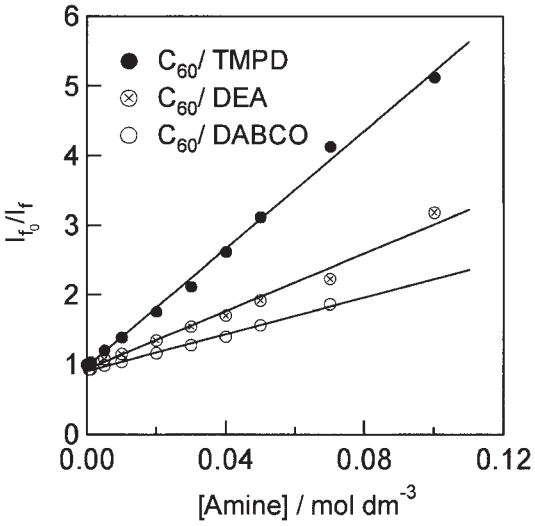

Fig. 3. Stern–Volmer plots for the fluorescence intensities (at 725 nm) of C_{60} in the presence of DEA, TMPD, and DABCO in toluene.

The possible processes after photoexcitation to $^1C_{60}$* are shown in Scheme 1 (reactions 2–6), in which the intersystem crossing (ISC) process to $^3C_{60}$* (reaction 2) competes with the fluorescence quenching (k_q^S[D]). As the fluorescence quenching processes, two processes are possible: one route is collisional quenching (k_{cq}^S) in reaction 3 and the other route is electron transfer (k_{et}^S; reactions 4–6). After the electron-transfer process, the radical ion-pair with singlet spin character is produced, from which three processes are possible; the first route is back electron transfer to the ground state within the radical ion pair (k_{bet}^{1st} in reaction 4), the second route is back electron transfer to $^3C_{60}$* within the radical ion pair ($k_{bet(T)}^{1st}$ in reaction 5), and the third route is dissociation into free radical ions (k_{diss}^S in reaction 6). The fractions among reactions 2–6 may depend on the donor strength, donor concentration, and solvent polarity.

Nanosecond Transient Absorption Measurements. Electron Transfer via $^3C_{60}$* with Donors in Polar Solvents: Transient absorption spectra observed by the nanosecond laser excitation of C_{60} in the presence of TMPD in BN are shown in Fig. 4. At low concentrations of TMPD (<20 mmol dm^{-3}), $^3C_{60}$* was observed at 740 nm immediately after the nanosecond laser excitation (532 nm light). Accompanying the decay of the 740 nm band of $^3C_{60}$*, the 1080 nm band due to $C_{60}^{\bullet-}$ grew up. The absorption band near 600 nm can be attributed to the radical cation of TMPD (TMPD$^{\bullet+}$).[28]

These observations indicate that intermolecular electron transfer takes place via $^3C_{60}$* in polar solvents, as shown in Scheme 2, when the concentration of amines is low. From the inserted time profiles in Fig. 4, the produced $C_{60}^{\bullet-}$ has a lifetime longer than several microseconds, suggesting the for-

Table 1. Oxidation Potentials of Amine Donors (E_{ox}) in BN and DCB and Rate Constants for Fluorescence Quenching of C_{60} (k_q^S) in Various Solvents

Donor	E_{ox}[a)]/V		k_q^S[b)]/mol^{-1} dm^3 s^{-1}		
	BN[c)]	DCB[c)]	BN[c)]	DCB[c)]	TN[c)]
DABCO	0.39	0.49	6.6×10^9	5.7×10^9	9.6×10^9
DEA	0.13	0.15	1.4×10^{10}	1.3×10^{10}	1.6×10^{10}
TMPD	−0.14	−0.08	2.7×10^{10}	3.1×10^{10}	3.3×10^{10}

a) E_{ox} is oxidation potential vs Fc/Fc$^+$. b) Each value contains the experimental error of ±5%; k_0^S (C_{60}) = 7.7×10^8 s^{-1} was employed in Eq. 1 in the text.[22] c) Solvent abbreviation, dielectric constant (ε_s) and viscosity (η) are (benzonitrile = BN, ε_s = 25.7, η = 1.24 cp), (*o*-dichlorobenzene = DCB, ε_s = 9.93, η = 1.32 cp), and (toluene = TN, ε_s = 2.38, η = 0.59 cp).[27]

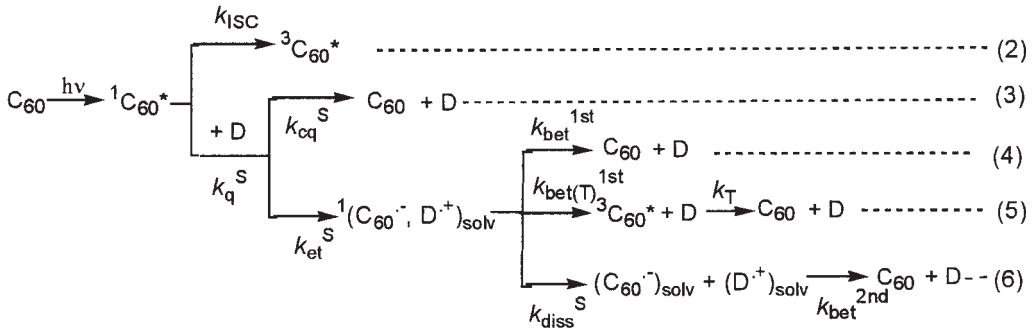

Scheme 1. Possible quenching processes via $^1C_{60}$* in the presence of donors (D).

mation of free radical ions (reaction 9) in BN. From the pseudo-first-order plots of the decay rate of $^3C_{60}$* and rise rate of $C_{60}^{\bullet-}$, the rate constants for the quenching (k_q^T) of $^3C_{60}$* with amines were evaluated, as listed in Table 2. The ratios of the maximal concentration of $C_{60}^{\bullet-}$ to the initial concentration of $^3C_{60}$* ($[C_{60}^{\bullet-}]_{max}/[^3C_{60}^*]_{intial}$) were calculated from the observed absorbance and reported molar extinction coefficients.[11,13,29] The plots of $[C_{60}^{\bullet-}]_{max}/[^3C_{60}^*]_{intial}$ vs amine donor concentrations show the saturation at ca. 20 mmol dm^{-3} of the amine donors. The saturated $[C_{60}^{\bullet-}]_{max}/[^3C_{60}^*]_{intial}$ values can be put equal to the quantum yields (Φ_{et}^T)[14,30] for electron transfer via $^3C_{60}$* (Table 2). The Φ_{et}^T values are all less than unity, suggesting that the collisional quenching of $^3C_{60}$* by amine donors occurs without electron transfer (reaction 7 in Scheme 2). The rate constants for electron transfer (k_{et}^T) from amines to $^3C_{60}$* were evaluated from the relation, $k_{et}^T = \Phi_{et}^T k_q^T$.[14,30] Finally, the k_{et}^T values were evaluated to be in the range of (1.9–5.0) $\times 10^9$ mol^{-1} dm^3 s^{-1}.

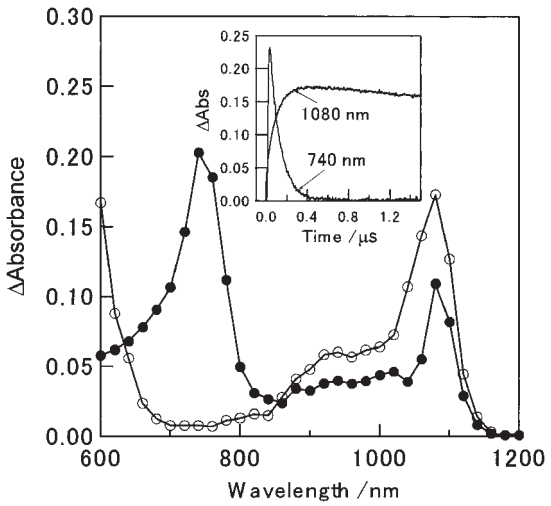

Fig. 4. Nanosecond transient absorption spectra of C_{60} (0.1 mmol dm^{-3}) in the presence of TMPD (1 mmol dm^{-3}) at 100 ns (●) and 1.0 μs (○) after 532 nm laser light irradiation in deaerated BN. Inset: Time profiles.

The k_{et}^T value for TMPD, which is close to the diffusion controlled limit in BN ($k_{diff} = 5.3 \times 10^9$ mol^{-1} dm^3 s^{-1}),[27] is the highest among three amines employed in the present study. This is supported by the most negative free-energy change ($\Delta G^\circ_{et}{}^T$) via $^3C_{60}$*, which was calculated by the Weller equation (Table 2).[31]

The absorption intensities of $[C_{60}^{\bullet-}]_{max}$ increase with the concentration of TMPD up to ca. 20 mmol dm^{-3} in BN, while $[C_{60}^{\bullet-}]_{max}$ begins to decrease in concentrations of TMPD higher than ca. 30 mmol dm^{-3}, as shown in Fig. 5(A). At 100 mmol dm^{-3}of TMPD, $[C_{60}^{\bullet-}]_{max}$ is about 40% to maximal $[C_{60}^{\bullet-}]_{max}$ at 20 mmol dm^{-3} of TMPD.

Since $C_{60}^{\bullet-}$ is generated by the electron transfer via $^3C_{60}$* produced by the ISC process from $^1C_{60}$*, the amounts of $[C_{60}^{\bullet-}]_{max}$ must be proportional to $[^3C_{60}^*]_{intial}$, which can be calculated by $k_0^S/(k_0^S + k_q^S[D])$. As shown in Fig. 5(B), the $[C_{60}^{\bullet-}]_{max}$ values for C_{60}–TMPD in BN decreased in concentrations higher than 20 mmol dm^{-3} along the curve calculated by $k_0^S/(k_0^S + k_q^S[D])$. Thus, the decrease in the $[C_{60}^{\bullet-}]_{max}$ values along $k_0^S/(k_0^S + k_q^S[D])$ suggests that dynamic quenching of $^1C_{60}$* takes place by the processes such as reactions 3 and 4 in Scheme 1, without generation of the radical ions observable in the time region longer than 6 ns (reaction 6 in Scheme 1). The processes of reaction 5 can be excluded from the main deactivation processes of a geminate radical ion-pair, since the regeneration of $^3C_{60}$* would reproduce $C_{60}^{\bullet-}$ and $TMPD^{\bullet+}$ keeping $[C_{60}^{\bullet-}]_{max}$ constant with increase in the TMPD concentration, which would cause considerable deviations from the calculated curve of Fig. 5(B).

If the generations of long-lived free radical-ions via $^1C_{60}$*

Table 2. Rate Constants for Quenching of $^3C_{60}$* with Amines (k_q^T) and Free-Energy Changes (ΔG_{et}^T), Quantum Yields (Φ_{et}^T), and Rate Constants (k_{et}^T) for Electron Transfer from Amines to $^3C_{60}$* in BN

Donor	$\Delta G^\circ_{et}{}^T$ a) /eV	k_q^T b) /mol^{-1} dm^3 s^{-1}	Φ_{et}^T b)	k_{et}^T b) /mol^{-1} dm^3 s^{-1}
DABCO	−0.37	3.2×10^9	0.60	1.9×10^9
DEA	−0.63	3.6×10^9	0.69	2.5×10^9
TMPD	−0.90	5.4×10^9	0.93	5.0×10^9

a) The $\Delta G^\circ_{et}{}^T$ values were calculated from the Rehm–Weller equation ($\Delta G^\circ_{et}{}^T = E_{ox}(D) - E_{red}(C_{60}) - E_T - E_c$),[30] employing the T_1-energy level (E_T) of $^3C_{60}$* (= 1.53 eV),[12] the reduction potential (E_{red}) of C_{60} (−1.05 V vs Fc/Fc$^+$),[3,4] and E_c (Coulomb energy) (= 0.06 eV) in BN.[12] b) Each value contains the experimental error of ±5%.

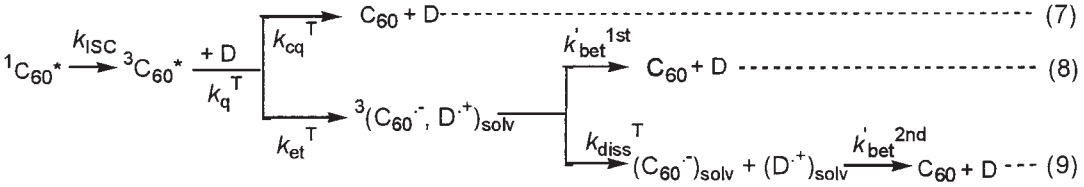

Scheme 2. Possible quenching routes of $^3C_{60}$* in the presence of donors (D).

are included, a monotonous increase in $[C_{60}^{\bullet-}]_{max}$ would be observable with an increase in TMPD. Therefore, the main reason for the unusual decrease of $[C_{60}^{\bullet-}]_{max}$ at higher donor concentration, even in highly polar solvents such as BN, is attributed to the fast back electron transfer within the geminate radical ion-pair keeping singlet spin character; i.e., ${k_{bet}}^{1st} > {k_{diss}}^{S}$.

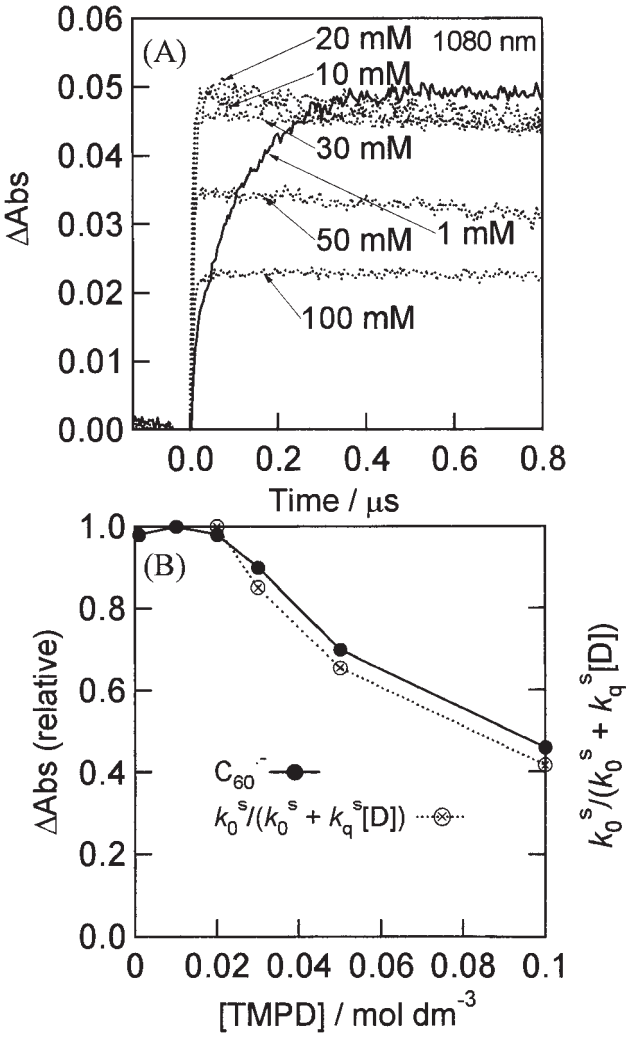

Fig. 5. (A) Absorbance time profiles of $C_{60}^{\bullet-}$ at 1080 nm at various TMPD concentrations in deaerated BN. (B) Plots of relative ΔAbs of $[C_{60}^{\bullet-}]_{max}$ at 1080 nm and ${k_0}^{S}/({k_0}^{S} + {k_q}^{S}[D])$ values against [TMPD] (= [D]); both values are normalized at [TMPD] = 20 mmol dm^{-3}.

Electron Transfer via $^3C_{60}$* in Intermediately Polar Solvents. In DCB which has intermediate polarity (dielectric constant (ε_s) = 9.93) between BN (ε_s = 25.7) and toluene (ε_s = 2.38), transient absorption spectra similar to Fig. 4 were observed, indicating electron transfer via $^3C_{60}$* producing $C_{60}^{\bullet-}$. The ${k_q}^{T}$, ${\Phi_{et}}^{T}$, and ${k_{et}}^{T}$ values are summarized in Table 3. The ${k_q}^{T}$ value for TMPD is almost the same as that in BN, while the ${k_q}^{T}$ values for DABCO and DEA are about a half of these values in BN. The ${\Phi_{et}}^{T}$ values for DABCO and TMPD in DCB are smaller than those in BN by factors of 20–40%. The ${\Phi_{et}}^{T}$ value for DEA was much smaller (ca. 1/10) than those of TMPD and DABCO in DCB. Thus, the ${k_{et}}^{T}$ values in DCB are smaller than those in BN. In DCB, collisional quenching without electron transfer via $^3C_{60}$* takes place more efficiently than in BN; especially, for DEA, $^3C_{60}$* was quenched predominantly by collisional quenching. Such small ${\Phi_{et}}^{T}$ values in DCB were reported for other aniline derivatives.[32]

The time profiles of $C_{60}^{\bullet-}$ at various DABCO concentrations are shown in Fig. 6(A). For DABCO and TMPD, decreases in $[C_{60}^{\bullet-}]_{max}$ with an increase in the donor concentration were observed. Decay rates of $C_{60}^{\bullet-}$ after reaching maxima in DCB are faster than those in BN. Faster decay of $C_{60}^{\bullet-}$ suggests appreciable interaction between $C_{60}^{\bullet-}$ and the donor radical cations in such intermediate polar solvents; i.e., ${k'_{bet}}^{1st} > {k_{diss}}^{T}$.

Since $[C_{60}^{\bullet-}]_{max}$ and ${k_0}^{S}/({k_0}^{S} + {k_q}^{S}[D])$ for the C_{60} and DABCO system in DCB decrease in concentrations higher than 20 mmol dm^{-3}, as shown in Fig. 6(B), $C_{60}^{\bullet-}$ is generated predominantly via $^3C_{60}$* (Scheme 2). Thus, this observation also suggests that fast back electron transfer (reaction 4) and collisional quenching of $^1C_{60}$* (reaction 3) in Scheme 1 take place in DCB; i.e., ${k_{bet}}^{1st} > {k_{diss}}^{S}$ and/or ${k_{cq}}^{S} > {k_{et}}^{S}$.

Electron Transfer via $^3C_{60}$* in Nonpolar Solvents. For TMPD in toluene, generation of $C_{60}^{\bullet-}$ was also confirmed, as shown in Fig. 7; however, the decay of $C_{60}^{\bullet-}$ completed within ca. 0.1–0.2 μs, which was as fast as the decay of $^3C_{60}$*. This suggests that photoinduced electron transfer takes place predominantly via $^3C_{60}$* producing radical ion-pair (RIP), which returns quickly to the neutral molecules in the ground states as shown in reaction 8 in Scheme 2; i.e., ${k'_{bet}}^{1st} > {k_{diss}}^{T}$ in toluene.

In toluene in the presence of DABCO, the generation of $C_{60}^{\bullet-}$ via $^3C_{60}$* was also observed; the decay of $C_{60}^{\bullet-}$ completed within 1.5 μs. $[C_{60}^{\bullet-}]_{max}$ increases until [DABCO] = 20 mmol dm^{-3}, while $[C_{60}^{\bullet-}]_{max}$ begins to decrease at concentrations higher than 20 mmol dm^{-3}. The decreasing curve of $[C_{60}^{\bullet-}]_{max}$ is in agreement with the calculated $[^3C_{60}^{*}]_{initial}$ by ${k_0}^{S}/({k_0}^{S} + {k_q}^{S}[D])$.

Table 3. Rate Constants for Quenching of $^3C_{60}$* (${k_q}^{T}$), and Free-Energy Changes (${\Delta G^\circ_{et}}^{T}$), Quantum Yields (${\Phi_{et}}^{T}$), and Rate Constants (${k_{et}}^{T}$) for Electron Transfer from Amines to $^3C_{60}$* in DCB

Donor	${\Delta G^\circ_{et}}^{T}$ a) /eV	${k_q}^{T}$ b) /mol^{-1} dm^3 s^{-1}	${\Phi_{et}}^{T}$ b)	${k_{et}}^{T}$ b) /mol^{-1} dm^3 s^{-1}
DABCO	−0.27	1.5×10^9	0.51	7.6×10^8
DEA	−0.61	1.9×10^9	0.06	1.1×10^8
TMPD	−0.84	6.0×10^9	0.52	3.1×10^9

a) ${\Delta G^\circ_{et}}^{T} = E_{ox}(D) - E_{red}(C_{60}) - E_T - E_c$.[30] b) Each value contains the experimental error of ±5%.

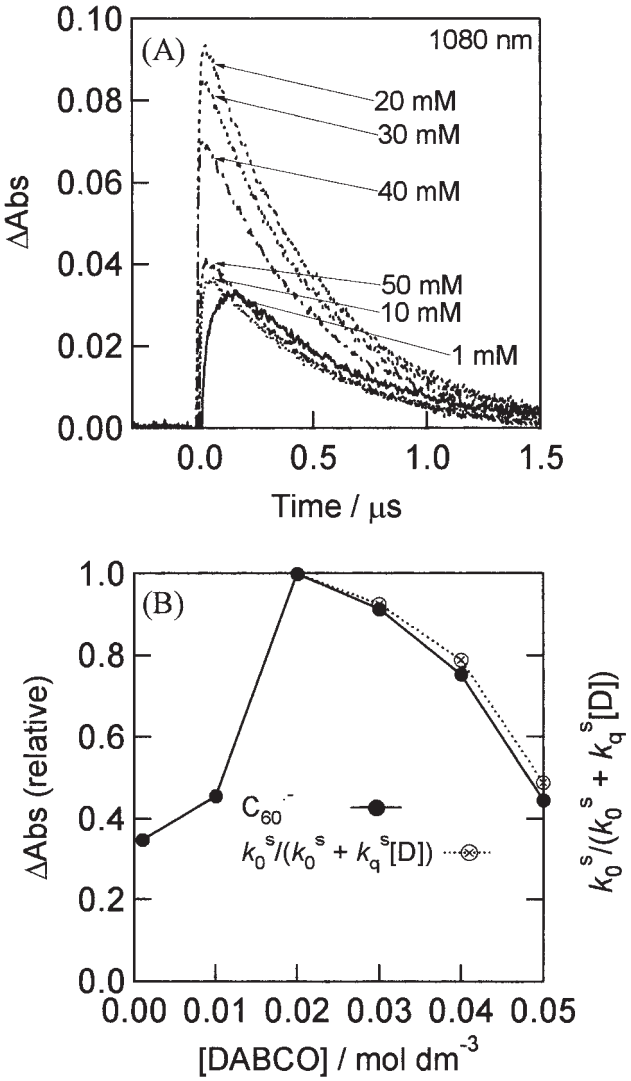

Fig. 6. (A) Absorbance time profiles of $C_{60}^{\bullet-}$ at 1080 nm at various DABCO concentrations (mM = mmol dm^{-3}) in the presence of C_{60} (0.1 mmol dm^{-3}) in deaerated DCB. (B) Relative ΔAbs of $[C_{60}^{\bullet-}]_{max}$ and $k_0^S/(k_0^S + k_q^S[D])$ values against [DABCO] (= [D]); both values are normalized at [DABCO] = 20 mmol dm^{-3}.

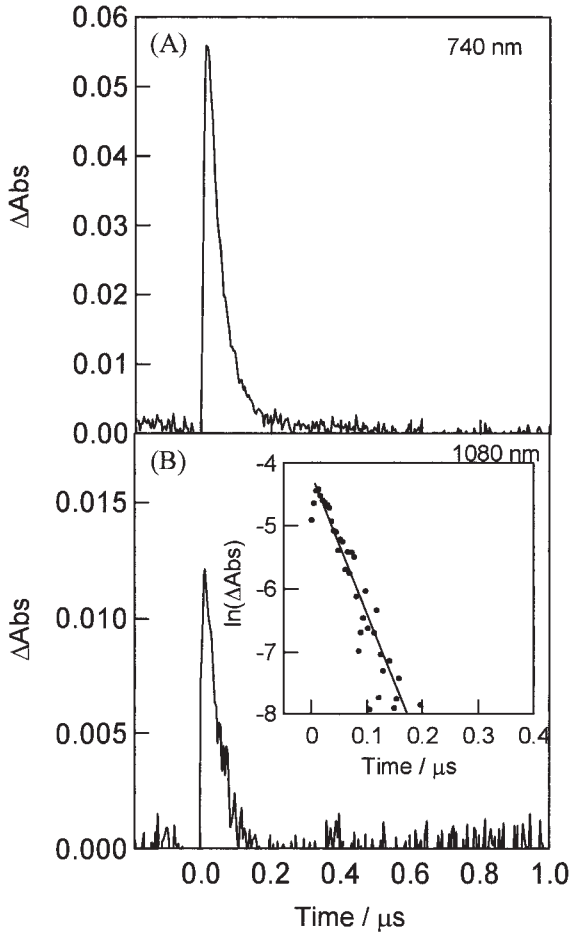

Fig. 7. Absorbance time profiles of C_{60} (0.1 mmol dm^{-3}) in the presence of TMPD (1 mmol dm^{-3}) at (A) 740 nm and (B) 1080 nm in deaerated toluene. Inset: Fast-order plot.

The k_q^T, Φ_{et}^T, and k_{et}^T values in toluene for three amine donors are summarized in Table 4. In the cases of TMPD and DABCO, fast electron transfer takes place even in toluene; however, the Φ_{et}^T values were not accurately evaluated, because the fast decay of $^3C_{60}^*$ affects $[^3C_{60}^*]_{initial}$, since it takes place within the laser light pulse duration.

In the case of DEA, evidence of electron transfer was not obtained, since no absorption of $C_{60}^{\bullet-}$ appeared in the 1000–1100 nm region even in the presence of high concentrations of DEA up to 100 mmol dm^{-3} as shown in Fig. 8. The inset of Fig. 8 shows the decay time profile of $^3C_{60}^*$ in the presence of a high concentration of DEA. From the slight increased decay rate of $^3C_{60}^*$, the bimolecular rate constant was evaluated to be 7×10^6 mol^{-1} dm^3 s^{-1}, which is an extremely slow quenching rate constant of $^3C_{60}^*$ compared with other electron donors in toluene.[11–16]

As shown in Fig. 9(A), an appreciable decrease in $[^3C_{60}^*]_{initial}$ was observed with an increase in concentration of DEA in toluene, indicating the presence of some process competitive with the ISC process (Scheme 1). The calculated $[^3C_{60}^*]_{initial}$ by $k_0^S/(k_0^S + k_q^S[D])$ decreases with an increase in [DEA], showing quite good agreement with the observed change of $[^3C_{60}^*]_{initial}$, as shown in Fig. 9(B). This finding indicates that $^3C_{60}^*$ is produced predominantly via ISC competing with the quenching processes of $^1C_{60}^*$ by DEA without forming prolong $C_{60}^{\bullet-}$ in toluene.

Rehm–Weller Plots. These k_q^T values are plotted vs ΔG°_{et}, as shown in Fig. 10, in which the k_q^T values for TMPD, DABCO, and DEA in BN, DCB, and toluene are almost along the curve expected by Rehm–Weller plot as shown in Fig. 10.[33] Collision between DEA and $^3C_{60}^*$ within a radius to quench the excited triplet energy of C_{60} in DCB is possible in the same way for other amine donors in other solvents. When similar plots were performed for the k_q^T values, deviation was observed for DEA in DCB, in which $k_{cq}^T \gg k_{et}^T$.

Back Electron Transfer. In toluene, the fast decay of $C_{60}^{\bullet-}$ resulting from recombination of $TMPD^{\bullet+}$ with $C_{60}^{\bullet-}$ produced via $^3C_{60}^*$ obeyed first-order kinetics, as shown in Fig. 7(B), indicating that back electron transfer occurs within the radical ion-pair. Since the decay rate of $C_{60}^{\bullet-}$ increased with an increase in the decay rate of $^3C_{60}^*$ under high TMPD

Table 4. Rate Constants for Quenching of $^3C_{60}$* (k_q^T) and Free-Energy Changes ($\Delta G^\circ_{et}{}^T$), Quantum Yields ($\Phi_{et}{}^T$), and Rate Constants ($k_{et}{}^T$) for Electron Transfer from Amines to $^3C_{60}$* in TN

Donor	$\Delta G^\circ_{et}{}^T$ a) /eV	k_q^T /10^9 mol^{-1} dm^3 s^{-1}	$\Phi_{et}{}^T$	$k_{et}{}^T$ /10^9 mol^{-1} dm^3 s^{-1}
DABCO	−0.07	3.6×10^9 b)	(0.5)c)	(1.8×10^9)d)
DEA	+0.21	7×10^6 b)	(0)	
TMPD	−0.23	7.5×10^9 b)	(0.3)c)	(2.3×10^9)d)

a) $\Delta G^\circ_{et}{}^T(TN) = \Delta G^\circ_{et}{}^T(BN) - \Delta G^\circ_s$, where $\Delta G^\circ_{et}{}^T(BN)$ was calculated from the Rehm–Weller equation ($\Delta G^\circ_{et}{}^T = E_{ox}(D) - E_{red}(C_{60}) - E_T - E_c$),[28] employing the T_1-energy level (E_T) of $^3C_{60}$* (= 1.53 eV),[11] the reduction potential (E_{red}) of C_{60} (−1.05 V vs Fc/Fc$^+$),[3,4] and E_c (Coulomb energy) (= 0.06 eV) in BN.[11] ΔG°_s was defined as $\Delta G^\circ_s = e^2/(4\pi\Delta\varepsilon_0)[(1/2R_+ + 1/2R_- - 1/R_{cc})1/\varepsilon_s - (1/2R_+ + 1/2R_-)1/\varepsilon_r]$, where R_+ and R_- are radii of the ion radicals of donors (2–5 Å) and C_{60} (4.7 Å), respectively; R_{cc} is the center-to-center distance between the two moieties (6–10 Å); ε_s and ε_r are static dielectric constants of solvents used for the rate measurements and the redox potential measurements, respectively. b) Each value contains the experimental error of ±5%. c) Difficult to estimate $[^3C_{60}*]_{initial}$, because of the rapid decay within the scattering of the laser light pulse (6 ns). d) Each value contains the experimental error of ±10%.

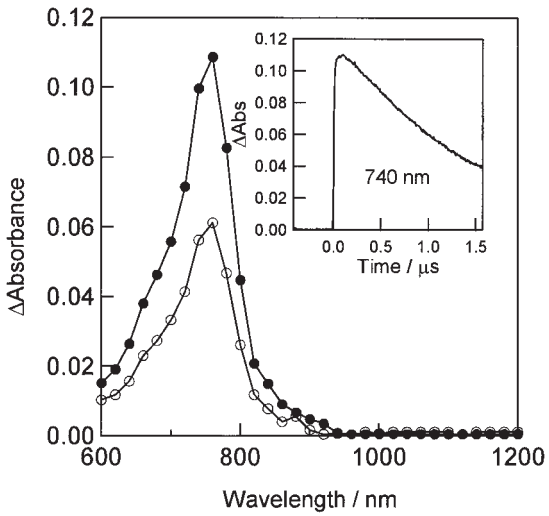

Fig. 8. Nanosecond transient absorption spectra of C_{60} (0.1 mmol dm^{-3}) in the presence of DEA (100 mmol dm^{-3}) at 100 ns (●) and 1.0 μs (○) after 532 nm laser light irradiation in deaerated toluene. Inset: Time profile at 740 nm.

concentration, back electron transfer must take place as soon as the radical ion-pair is produced; i.e., $k'_{bet}{}^{1st} > k_{et}{}^T$[TMPD] in the region of 50–100 mmol dm^{-3} of TMPD. Table 5 lists the $k'_{bet}{}^{1st}$ value for TMPD in toluene with the highest donor concentration; such a $k'_{bet}{}^{1st}$ value is still regarded as the lowest limit. The $k'_{bet}{}^{1st}$ value in the order of 10^7 s^{-1} suggests that $C_{60}{}^{\bullet-}$–TMPD$^{\bullet+}$ is present as a contact radical ion-pair. Similarly, $C_{60}{}^{\bullet-}$ for recombination with DABCO$^{\bullet+}$ also decayed according to first-order kinetics; however, the $k'_{bet}{}^{1st}$ value for DABCO$^{\bullet+}$ is one order smaller than that of recombination with TMPD$^{\bullet+}$. The bulkiness of DABCO may loosen the radical ion-pair even in toluene.

In DCB, the decay time profiles of $C_{60}{}^{\bullet-}$ for recombination with DABCO$^{\bullet+}$ (Fig. 6(A)) and that with DEA$^{\bullet+}$ produced via $^3C_{60}$* obey a single exponential, similar to those in toluene. The same $k'_{bet}{}^{1st}$ value for $C_{60}{}^{\bullet-}$–DABCO$^{\bullet+}$ in DCB and toluene suggests that DABCO$^{\bullet+}$–$C_{60}{}^{\bullet-}$ in DCB is present as a radical ion-pair similar to that in toluene. On the other hand, the $k'_{bet}{}^{1st}$ value for $C_{60}{}^{\bullet-}$–DEA$^{\bullet+}$ is smaller than that for

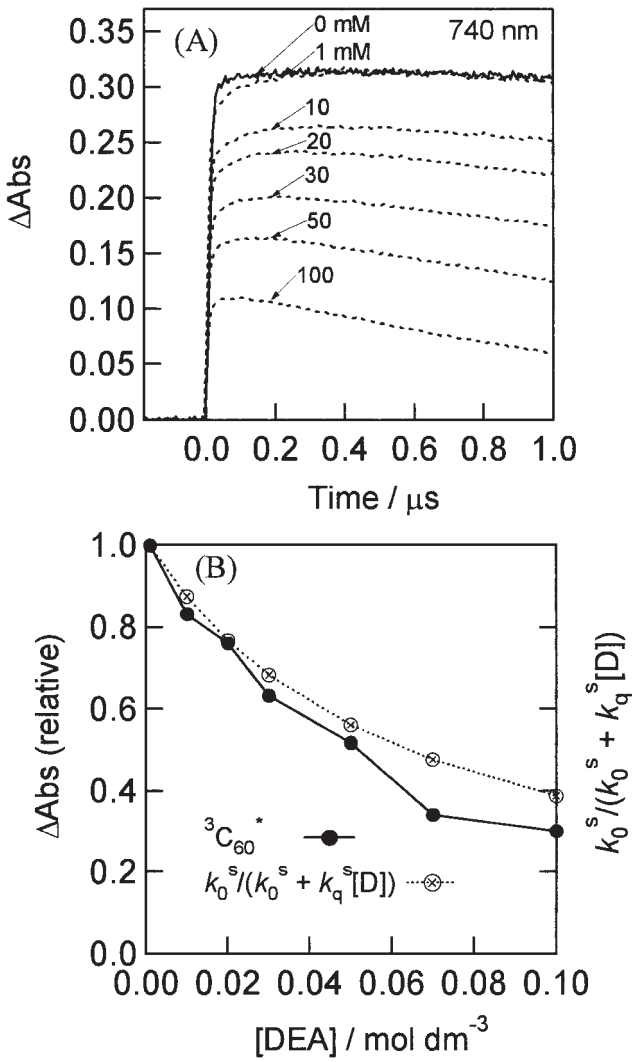

Fig. 9. (A) Time profiles of the absorbance at 740 nm of $^3C_{60}$* in the presence of DEA at various concentration in deaerated toluene (mM = mmol dm^{-3}). (B) Plots of relative absorbance of $[^3C_{60}*]_{intial}$ at 740 nm and $k_0{}^S/(k_0{}^S + k_q{}^S[D])$ values against [DEA] (= [D]). Both values are normalized at [DEA] = 0.

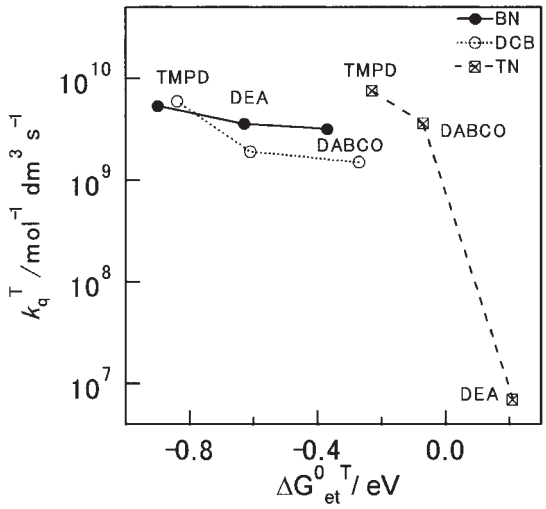

Fig. 10. Rehm–Weller plots for $k_q{}^T$ vs $\Delta G^\circ{}_{et}{}^T$.

$C_{60}{}^{\bullet-}$–$DABCO^{\bullet+}$ by a factor of ca. 1/10, suggesting that $DEA^{\bullet+}$–$C_{60}{}^{\bullet-}$ is present as a loose radical ion-pair such as the solvent-separated radical ion-pair (SSRIP) in DCB. For $C_{60}{}^{\bullet-}$–$TMPD^{\bullet+}$ in DCB, the time profile of $C_{60}{}^{\bullet-}$ consists of two components, in which each component obeys first-order kinetics, as shown in the inset of Fig. 11(A). From the fast decay component (0–1 μs), the $k'_{bet}{}^{1st}$ value was evaluated as 5.2×10^6 s^{-1}, which is greater than that of DABCO in toluene, suggesting that back electron transfer takes place within the contact radical ion-pair. From the slow part (1–20 μs), the $k'_{bet}{}^{1st}$ value was evaluated as 2.4×10^5 s^{-1}, which suggests back electron transfer within SSRIP in DCB. These observations indicate that there are two kinds of radical ion-pairs for $TMPD^{\bullet+}$–$C_{60}{}^{\bullet-}$ in DCB.

In BN, the decays of $C_{60}{}^{\bullet-}$ obey second-order kinetics (Fig. 11(B)), suggesting that the radical ions produced via $^3C_{60}$* are separately solvated, yielding free radical ions. The bimolecular back electron-transfer rate-constants ($k'_{bet}{}^{2nd}$) of the radical ions produced via $^3C_{60}$* were evaluated from the slope of the second-order plots ($k'_{bet}{}^{2nd}/\varepsilon$) on substituting the reported molar extinction coefficients (ε) for $C_{60}{}^{\bullet-}$.[29] The evaluated $k'_{bet}{}^{2nd}$ values are summarized in Table 5. These values are close to the diffusion controlled limit ($k_{diff} = 5.3 \times 10^9$ mol^{-1} dm^3 s^{-1})[27] in BN.

It is also notable that the $k'_{bet}{}^{1st}$ value for $DEA^{\bullet+}$–$C_{60}{}^{\bullet-}$ is smaller than those for $DABCO^{\bullet+}$–$C_{60}{}^{\bullet-}$ and $TMPD^{\bullet+}$–$C_{60}{}^{\bullet-}$ in DCB, which may give a hint to interpret the extremely small $\Phi_{et}{}^T$ and $k_{et}{}^T$. Collision between DEA and $^3C_{60}$* within a radius to consume the excited triplet energy of C_{60} in DCB is possible, but electron transfer is prohibited in DCB and toluene. Since the radical ion-pair ($DEA^{\bullet+}$–$C_{60}{}^{\bullet-}$) is the loosest in DCB, there may be a specific reason that DEA can not approach $^3C_{60}$* within a radius between DEA and $^3C_{60}$* which would lead to electron transfer.[34] Such a specific behavior of DEA in DCB was not observed in highly polar BN.

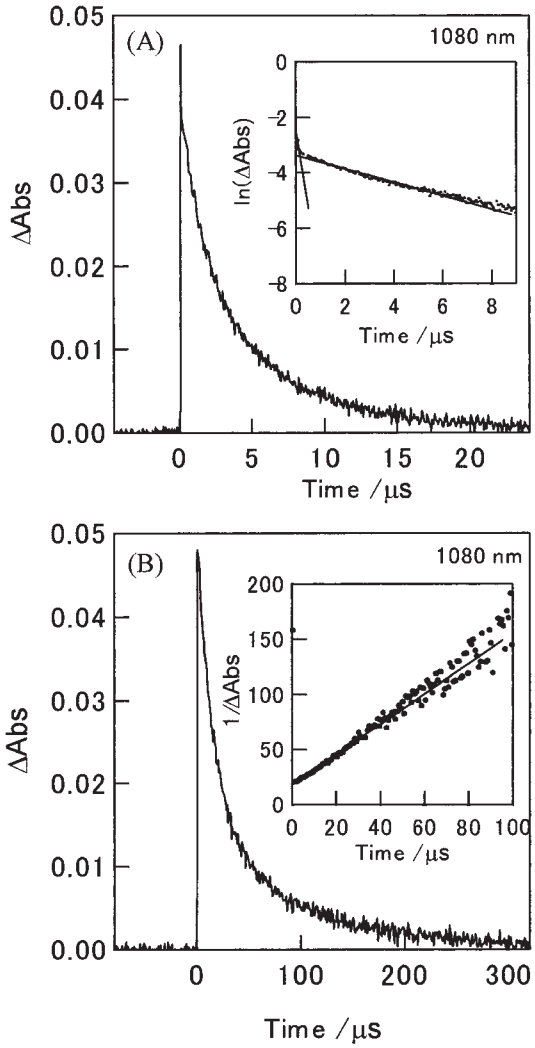

Fig. 11. Long time decay profiles of $C_{60}{}^{\bullet-}$ at 1080 nm in the presence of equimolar $TMPD^{\bullet+}$ in (A) DCB and (B) BN. Inset of (A): First-order plot for decay of $C_{60}{}^{\bullet-}$ in DCB. Inset of (B): Second-order plot for decay of $C_{60}{}^{\bullet-}$ in BN.

Table 5. Rate Constants ($k'_{bet}{}^{2nd}$ and $k'_{bet}{}^{1st}$)[a] and Free-Energy Changes ($\Delta G^\circ{}_{bet}$) for Back Electron Transfer from $C_{60}{}^{\bullet-}$ to $D^{\bullet+}$ [b]

Donor	$k'_{bet}{}^{2nd}$ ($\Delta G^\circ{}_{bet}$/eV) /mol^{-1} dm^3 s^{-1} in BN	$k'_{bet}{}^{1st}$ ($\Delta G^\circ{}_{bet}$/eV) /s^{-1} in DCB	$k'_{bet}{}^{1st}$ ($\Delta G^\circ{}_{bet}$/eV) /s^{-1} in TN
DABCO	5.0×10^9 (−1.13)	1.3×10^6 (−1.23)	1.6×10^6 (−1.43)
DEA	5.1×10^9 (−0.97)	7.0×10^4 (−0.89)	— (−1.77)
TMPD	8.1×10^9 (−0.40)	5.2×10^6 [c] (−0.66) 2.4×10^5 [d]	2.2×10^7 (−1.27)

a) The reported ε value (12000 cm^{-1} mol^{-1} dm^3 for $C_{60}{}^{\bullet-}$ at 1080 nm)[29] was employed for the calculations of $k'_{bet}{}^{2nd}$. b) ΔG_{bet} values were calculated from $\Delta G^\circ{}_{bet} = E_{ox}(D) - E_{red}(C_{60}) - E_c - \Delta G^\circ{}_s$ (see caption of Table 4).[31] c) From fast decay part. d) From slow decay part.

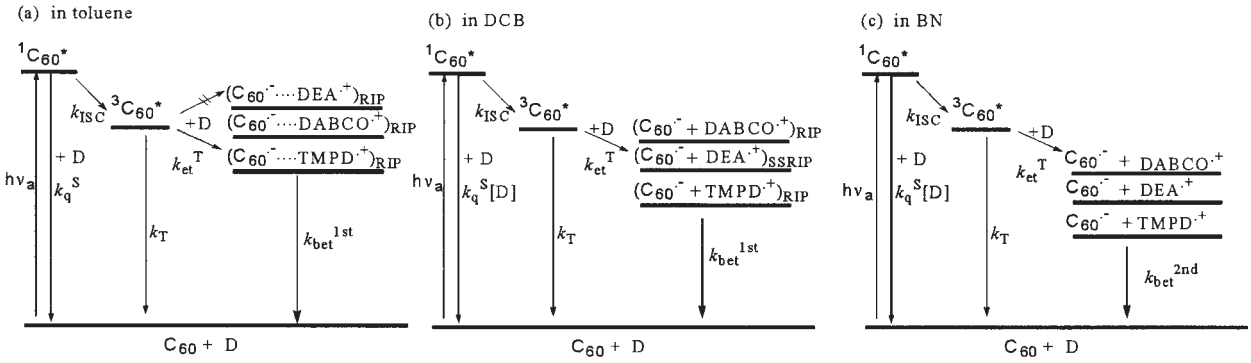

Fig. 12. Energy diagrams for three donors in three solvents.

Energy Diagrams. Energy diagrams for photoinduced electron transfer are schematically illustrated in Fig. 12. For all cases, $^3C_{60}$* is generated via $^1C_{60}$* by ISC competing with the quenching processes of $^1C_{60}$* (k_q^S[D]).

In toluene, electron transfer from DEA to $^3C_{60}$* is endothermic; thus, the slow quenching of $^3C_{60}$* predominates deactivation processes, generating the ground state of C_{60} without formation of the radical ion-pair. For DABCO and TMPD, the radical ion-pairs are produced via $^3C_{60}$* because of the exothermic process; the radical ion-pair may be strongly contacting for TMPD in toluene, as indicated by the quick first-order decay of $C_{60}^{\bullet-}$. In DCB, the electron-transfer process via $^3C_{60}$* is also exothermic; thus, electron transfer from DABCO and TMPD to $^3C_{60}$* occurs effectively, generating a radical ion-pair. Electron transfer from DEA to $^3C_{60}$* becomes also exothermic, although the efficiency is low. In BN, the electron-transfer process via $^3C_{60}$* is further exothermic, giving high Φ_{et}^T and large k_{et}^T; since the radical ions are separately solvated in BN, the radical ions persist as long as several hundred microseconds.

Thermodynamically, it is anticipated that electron transfer via $^1C_{60}$* is rather more favorable for these three amine donors in all solvents than that via $^3C_{60}$*. The free energy changes via $^1C_{60}$* ($\Delta G^\circ_{et}{}^S$) are ca. 0.2 eV more negative than those via $^3C_{60}$* ($\Delta G^\circ_{et}{}^T$), since the energy difference between S_1 and T_1 is ca. 0.2 eV.[11] However, for all donors in all solvents, no evidence for electron transfer via $^1C_{60}$* was observed by our nanosecond transient absorption measurements using a laser light pulse (6 ns). Even if electron transfer takes place via $^1C_{60}$* in polar BN, all processes via $^1C_{60}$* finished within nanosecond time region less than ca. 6 ns; that is, $k_{bet}^{1st} \gg k'_{bet}{}^{1st}$ and $k_{bet}^{2nd} \gg k'_{bet}{}^{2nd}$.

In the case of DEA in toluene, the energy level of the radical ion-pair is between the energy levels of $^1C_{60}$* and $^3C_{60}$*. If a short-lived radical ion-pair ($C_{60}^{\bullet-}$, $DEA^{\bullet-})_{solv}$ is produced via $^1C_{60}$*, $^3C_{60}$* is possibly reproduced by rapid back electron transfer within the radical ion-pair. If so, it would be anticipated that the decrease in $^3C_{60}$* would not be observed. Thus, Fig. 9(B) indicates that the process via $^1C_{60}$* is attributed to predominant collisional quenching without electron transfer.

Comparison with Reported Observations. Interactions between amines and C_{60} in the ground and excited states were frequently reported in the literature, when the concentrations of the amine donors are higher than 1000 mmol dm^{-3}.[26] In the present study for the intermediate concentration region until 100 mmol dm^{-3}, we clarified that appreciable interaction between amines and C_{60} in the ground and excited states is absent. When the concentrations of the amine donors are less than 10 mmol dm^{-3}, photoinduced electron-transfer processes via $^3C_{60}$* have predominantly been reported.[11–18]

In non-polar solvents, fast electron transfer with quick back electron transfer within the picosecond time scale was reported for amine donor concentrations higher than 1000 mmol dm^{-3};[7–9] in this case, forward and backward electron transfer may occur within the excited charge-transfer (CT) complexes. Thus, it is impossible to directly compare these reported phenomena with our observations, which were performed under the conditions where such CT complexes are not appreciably present in nonpolar solvent. In the intermediate concentration region until 100 mmol dm^{-3}, we obtained evidence that the radical ion-pairs are generated via $^3C_{60}$* with lifetimes observable by nanosecond laser photolysis, while no trace of the radical ion-pairs was observed via $^1C_{60}$* in time regions longer than ca. 6 ns. These findings suggest that $k_{bet}^{1st} > k'_{bet}{}^{1st}$ and/or $k_{cq}^S > k_{et}^S$.

In polar solvents, on the other hand, photoinduced processes in intermediate concentrations of donors have not been extensively reported. From our observations in BN, we must consider that $C_{60}^{\bullet-}$ generated via $^1C_{60}$* exists as a geminate radical ion-pair, which quickly returns to neutral molecules in the ground states. Thus, $C_{60}^{\bullet-}$ does not survive longer than the duration of a nanosecond laser light pulse (6 ns). On the other hand, the radical ion-pairs generated via $^3C_{60}$* have a long lifetime to dissociate into free radical ions, because of the triplet spin character of the radical ion-pair. Thus, $k_{diss}^S < k_{bet}^{1st}$ in Scheme 1, while $k_{diss}^T > k'_{bet}{}^{1st}$ in Scheme 2. Therefore, for the observations of free radical ions with long lifetime in highly polar BN, the spin character of the radical ion-pair plays an important role even in polar solvents.

Conclusion

On combination of fluorescence quenching experiments and nanosecond transient absorption measurements, information about intermolecular electron transfer from various amine donors to $^1C_{60}$* and to $^3C_{60}$* has been obtained in various solvents. With increases in concentrations of amine donors, $[C_{60}^{\bullet-}]_{max}$ observed at times longer than 6 ns decreased even in highly polar solvent. This decrease in $[C_{60}^{\bullet-}]_{max}$ clearly accords with the decrease in $[^3C_{60}*]_{initial}$ via ISC from $^1C_{60}$*, which was consumed by amines. This suggests that the quenching of $^1C_{60}$* with the amine donors does not contribute to the

generation of persistent $C_{60}^{\bullet-}$, even in highly polar solvents.

This work was partly supported by JSPS: Grants-in-Aid for Scientific Researches (Nos. 10207202, 11740380, and 12875163). The authors are also grateful to the reviewers of this journal for their important comments.

References

1 K. Prassides, "Physics and Chemistry of the Fullerenes," NATO ASI Series, Kluwer Academic Publisher, Dordrecht (1994), Vol. C-443.

2 "Fullerene, Chemistry, Physics and Technology," ed by K. M. Kadish and R. S. Ruoff, Wiley-Interscience, New York (2000).

3 P. M. Allemand, A. Koch, F. Wudl, Y. Rubin, F. Diederich, M. M. Alvarez, S. J. Anz, and R. L. Whetten, *J. Am. Chem. Soc.*, **113**, 1050 (1991).

4 D. Dubois, K. M. Kadish, S. Flanagan, R. E. Haufler, L. P. F. Chibante, and L. J. Wilson, *J. Am. Chem. Soc.*, **114**, 4364 (1992).

5 M. Maggini and D. M. Guldi, "Molecular and Supramolecular Photochemistry," ed by V. Ramamurthy and K. S. Schanze, Marcel Dekker, New York (2000), Vol. 4, pp. 149–196.

6 D. M. Guldi and M. Prato, *Acc. Chem. Res.*, **33**, 695 (2000).

7 R. J. Sension, A. Z. Szarka, G. R. Smith, and R. M. Hochstrasser, *Chem. Phys. Lett.*, **185**, 179 (1991).

8 D. K. Palit, H. N. Ghosh, H. Pal, A. V. Sapre, J. P. Mittal, R. Seshadri, and C. N. R. Rao, *Chem. Phys. Lett.*, **198**, 113 (1992).

9 J. Park, D. Kim, Y. D. Suh, and S. K. Kim, *J. Phys. Chem.*, **98**, 12715 (1994).

10 I. Suzuki, Y. Tsuboi, H. Miyasaka, and A. Itaya, *Bull. Chem. Soc. Jpn.*, **73**, 589 (2000).

11 J. W. Arbogast, A. O. Darmanyan, C. S. Foote, Y. Rubin, F. N. Diederich, M. M. Alvarez, S. J. Anz, and R. L. Whetten, *J. Phys. Chem.*, **95**, 11 (1991).

12 J. W. Arbogast, C. S. Foote, and M. Kao, *J. Am. Chem. Soc.*, **114**, 2277 (1992).

13 L. Biczok, H. Linschitz, and R. I. Water, *Chem. Phys. Lett.*, **195**, 339 (1992).

14 C. A. Steren, H. van Willigen, L. Biczok, N. Gupta, and H. Linschitz, *J. Phys. Chem.*, **100**, 8920 (1996).

15 O. Ito, *Res. Chem. Intermed.*, **23**, 389 (1997).

16 A. Watanabe and O. Ito, *J. Phys. Chem.*, **98**, 7736 (1994).

17 O. Ito, Y. Sasaki, Y. Yoshikawa, and A. Watanabe, *J. Phys. Chem.*, **99**, 9838 (1995).

18 M. M. Alam, A. Watanabe, and O. Ito, *Bull. Chem. Soc. Jpn.*, **70**, 1833 (1997).

19 R. J. Sension, C. M. Phillips, A. Z. Szarka, W. J. Romanow, A. R. McGhie, J. P. McCauley, A. B. Smith, and R. M. Hochstrasser, *J. Phys. Chem.*, **95**, 6075 (1991).

20 T. W. Ebbesen, K. Tanigaki, and S. Kuroshima, *Chem. Phys. Lett.*, **181**, 501 (1991).

21 M. Lee, O.-K. Song, J.-C. Seo, D. Kim, Y. D. Suh, S. M. Jin, and S. K. Kim, *Chem. Phys. Lett.*, **196**, 325 (1992).

22 A. Watanabe, O. Ito, M. Watanabe, H. Saito, and M. Koishi, *Chem. Commun.*, **1996**, 117.

23 A. Itaya, I. Suzuki, Y. Tsuboi, and H. Miyasaka, *J. Phys. Chem. B*, **101**, 5118 (1997).

24 A. Masuhara, M. Fujitsuka, and O. Ito, *Bull. Chem. Soc. Jpn.*, **73**, 2199 (2000).

25 M. C. Rath, H. Pal, and T. Mukherjee, *J. Phys. Chem. A*, **103**, 4993 (1999).

26 Y. P. Sun, C. E. Bunker, and B. Ma, *J. Am. Chem. Soc.*, **116**, 9692 (1994).

27 S. I. Murov, I. Carmichael, and G. L. Hug, "Handbook of Photochemistry," Marcel-Dekker, New York (1993).

28 M. Fujitsuka, C. Luo, O. Ito, Y. Murata, and K. Komatsu, *J. Phys. Chem. A*, **103**, 7155 (1999).

29 G. A. Heath, J. E. McGrady, and R. L. Marín, *J. Chem. Soc., Chem. Commun.*, **1992**, 1272.

30 M. M. Alam, A. Watanabe, and O. Ito, *J. Photochem. Photobiol., A*, **104**, 59 (1997).

31 A. Weller, *Z. Phys. Chem., Neue Folge*, **133**, 93 (1982).

32 S. Komamine, M. Fujitsuka, and O. Ito, *Phys. Chem. Chem. Phys.*, **1**, 4745 (1999).

33 D. Rehm and A. Weller, *Isr. J. Chem.*, **8**, 259 (1970).

34 Steric reason can be excluded, since the same tendency was observed for unsubstituted aniline.[32]